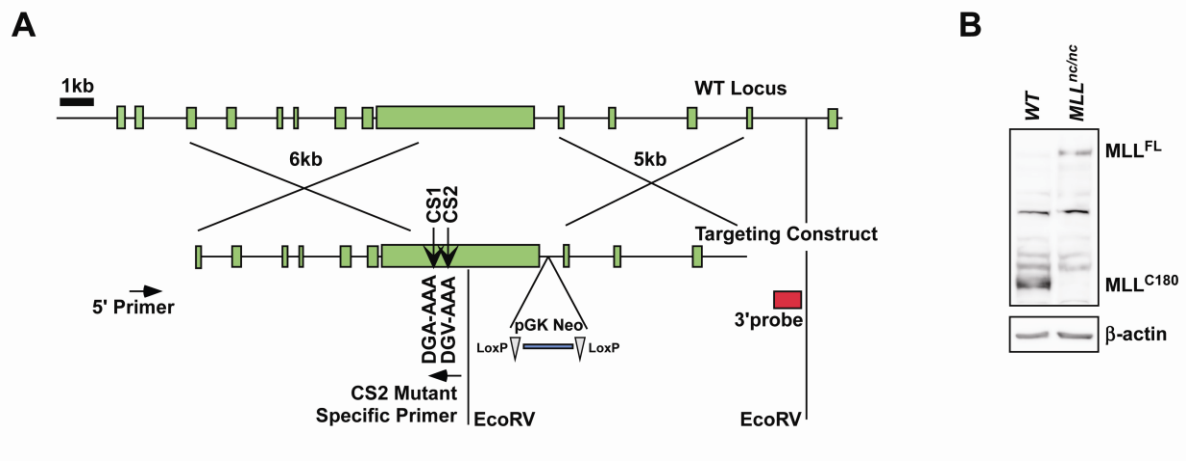

Figure S1

Generation of *MLL*$^{nc/nc}$ mice. (**A**) Schematics of the murine *MLL* genomic locus and the targeting construct carrying mutant Taspase1 cleavage site 1 and 2 (CS1 & CS2). The targeted allele was first derived in ES cells by homologous recombination, followed by transient expression of Cre recombinase to remove the Neo cassette, creating the *MLL non-cleavable (MLL*^{nc}*)* allele. (**B**) Cell lysates of *wild-type* (*WT*) and *MLL*$^{nc/nc}$ embryos (E10.5) were analyzed by the anti-MLL^{C180} Western blot.

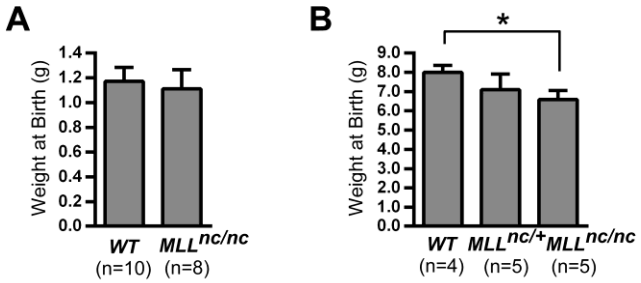

Figure S2

Body weight of *MLL*$^{nc/nc}$ mice. *WT* and *MLL*$^{nc/nc}$ mice were weighed at birth (**A**) and 3 weeks after birth (**B**). *MLL*$^{nc/nc}$ mice are significantly smaller than *WT* mice at 3 weeks of age. Data presented are mean ± SD.*$p < 0.05$.

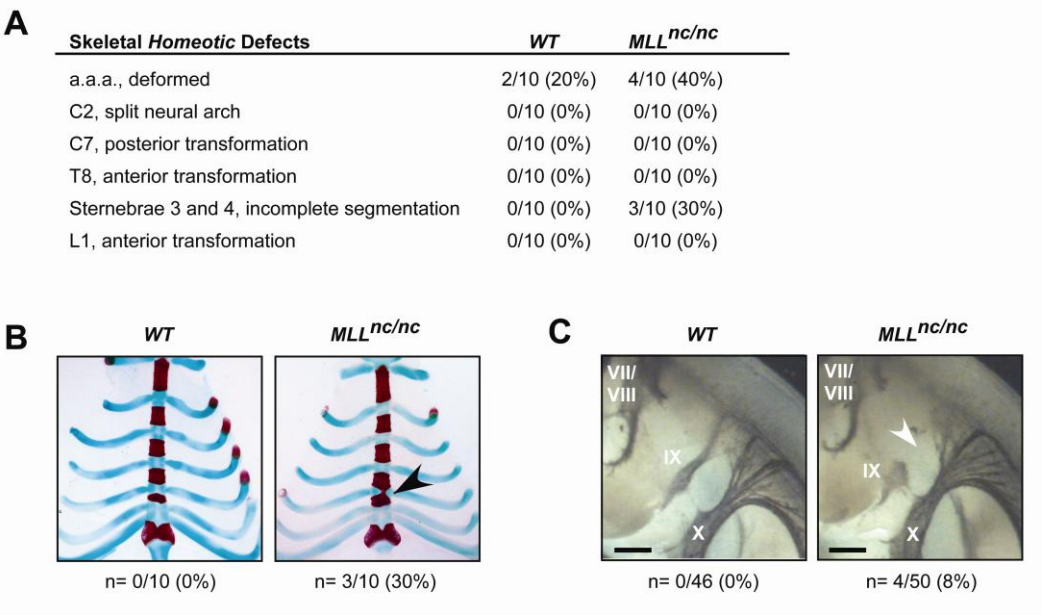

Figure S3

Homeotic defects of *MLL*$^{nc/nc}$ mice. (**A**) Summary of analysis on the skeletal development of *WT* and *MLL*$^{nc/nc}$ newborn mice. The numbers of animals exhibiting the indicated *homeotic* defects are displayed. a.a.a., anterior arch of atlas; C, cervical vertebra; T, thoracic vertebra; L, lumbar vertebra. (**B**) Ventral views of thoracic skeleton with ribs and sternebrae are presented. Newborn mice of the indicated genotypes were stained with Alizarin Red and Alcian Blue to visualize bone in red and cartilage in blue, respectively. The arrowhead indicates the incomplete segmentation between sternebra 3 and 4 in *MLL*$^{nc/nc}$ mice. (**C**) Neurofilament staining indicates patterning defects of CNIX in *MLL*$^{nc/nc}$ embryos. Lateral views of E10.5 embryos stained by whole mount immunohistochemistry using 2H3 anti-neurofilament antibody are presented. Facial (CNVII), acoustic (CNVIII), glossopharyngeal (CNIX), and vagal (CNX) nerves are shown. White arrowhead indicates the missing connection between the proximal and distal ganglia of the CNIX in *MLL*$^{nc/nc}$ embryos. Scale bar = 0.2 mm.

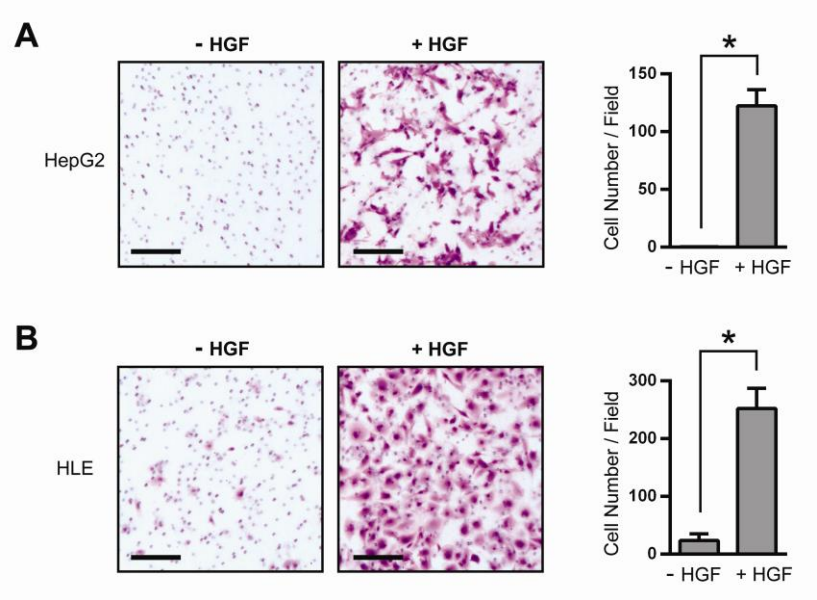

Figure S4

HGF induces HepG2 and HLE cells to invade through Matrigel-coated transwells. HepG2 (**A**) and HLE cells (**B**) were seeded on Matrigel-coated transwells and subjected to 20ng/ml and 50ng/ml HGF, respectively, for 24 hours. Invaded cells were stained with crystal violet and Hoechst 33342. Cell numbers were calculated from five independent fields of three independent experiments and presented as mean ± SD. *$p < 0.05$.

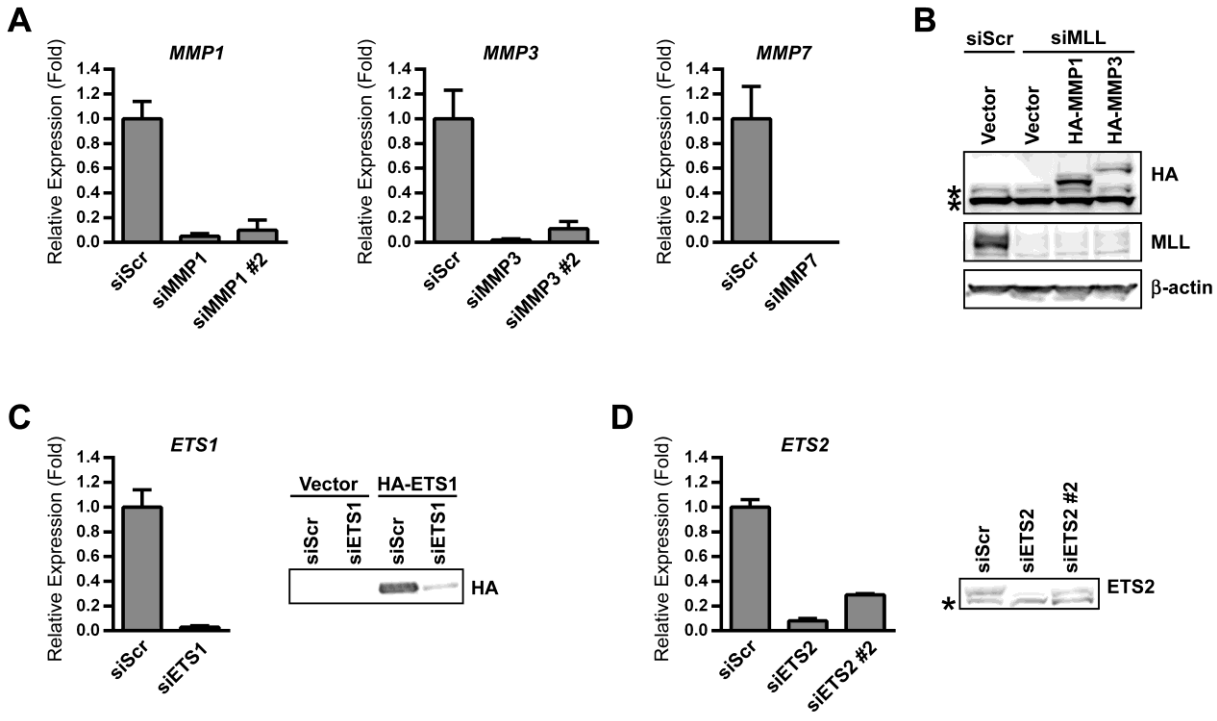

Figure S5

(**A**) The efficacy of siRNA-mediated knockdown of *MMP1*, *MMP3*, and *MMP7* in HepG2 cells are demonstrated by quantitative RT-PCR assays. (**B**) Immunoblots displaying overexpression of HA-tagged MMP1 and MMP3 and siRNA-mediated depletion of MLL in HepG2 cells. Non-specific cross-reactive bands denoted by asterisk. (**C**) *ETS1* knock-down by siRNA is exhibited by qRT-PCR and immunoblots. For the immunoblot, ETS1 was transiently overexpressed before knock-down, as endogenous ETS1 was below detectable levels. (**D**) *ETS2* knock-down by siRNA is exhibited by qRT-PCR and immunoblots. Non-specific cross-reactive bands denoted by asterisk. qRT-PCR data presented are mean ± SD from three independent experiments.